Effect of Sintering Temperature on the Photocatalytic Activities and Stabilities of Hematite and Silica-Dispersed Hematite Particles for Organic Degradation in Aqueous Suspensions

ARTICLE *in* LANGMUIR · APRIL 2009

Impact Factor: 4.46 · DOI: 10.1021/la803714m · Source: PubMed

3 AUTHORS, INCLUDING:

Weiping Du
Donghua University
14 PUBLICATIONS **326** CITATIONS
SEE PROFILE

Yiming Xu
Zhejiang University
64 PUBLICATIONS **2,252** CITATIONS
SEE PROFILE

Article

Effect of Sintering Temperature on the Photocatalytic Activities and Stabilities of Hematite and Silica-Dispersed Hematite Particles for Organic Degradation in Aqueous Suspensions

Yan Wang, Weiping Du, and Yiming Xu

Langmuir, **2009**, 25 (5), 2895-2899• DOI: 10.1021/la803714m • Publication Date (Web): 06 February 2009

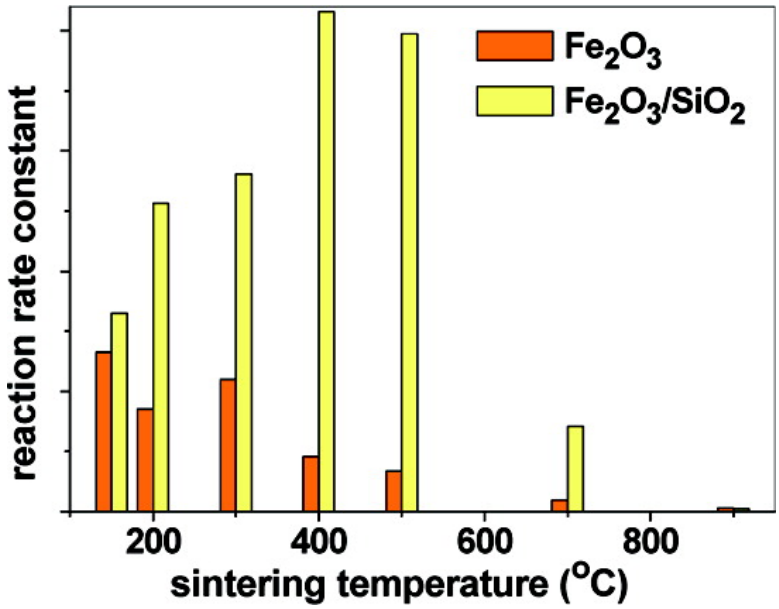

More About This Article

Additional resources and features associated with this article are available within the HTML version:

- Supporting Information
- Access to high resolution figures
- Links to articles and content related to this article
- Copyright permission to reproduce figures and/or text from this article

View the Full Text HTML

Effect of Sintering Temperature on the Photocatalytic Activities and Stabilities of Hematite and Silica-Dispersed Hematite Particles for Organic Degradation in Aqueous Suspensions

Yan Wang, Weiping Du, and Yiming Xu*

Department of Chemistry, Zhejiang University, Hangzhou 310027, China

Received November 9, 2008. Revised Manuscript Received January 5, 2009

The effect of sintering temperature (150−900 °C) on the photocatalytic activities of ferric oxide and silica-supported ferric oxide for Orange II degradation in water has been examined under UV light irradiation in the absence and presence of H_2O_2. The solids are characterized by X-ray powder diffraction, nitrogen adsorption, UV/vis diffuse reflectance spectroscopy, FTIR, and Raman spectroscopy. It was observed that the amount of dye adsorbed and the rate of dye photodegradation on these catalysts were a function of sintering temperature and the suspension pH. Evidence appears to correlate with the crystallinity, particle size, and flat-band potential of hematite, in agreement with the model of semiconductor photocatalysis. The recycling experiment showed that bare hematite was relatively stable, whereas silica-supported ferric oxide experienced a progressive degradation, due to preferential deposition of the dissolved ferric species onto silica, possibly with formation of amorphous and low photoactive ferric (hydr)oxide.

1. Introduction

Ferric oxide and oxyhydroxide are widespread in the natural environment.[1] Under sunlight irradiation, these minerals are known to undergo reductive dissolution into ferrous species, with concomitant oxidation of water or organic compounds at the solid−liquid interface.[2] From an environmental point of view, these photoreactions may be applicable for wastewater treatment. In fact, there have been several reports using ferric (hydr)oxides as a photocatalyst for pollutant degradation in aqueous suspension, of such pollutants as sulfur dioxide,[3] carboxylic acid,[4−7] substituted phenols,[8−11] azo dyes,[12,13] and benzothiazole.[14] In those reports, the importance of substrate preadsorption on the catalyst surface is emphasized, and the reactions are largely interpreted either by a photoinduced ligand-to-metal charge transfer (LMCT) within a surface complex or by a band gap excitation of semiconductors. We have recently proposed[15] that ferric (hydr)oxide-mediated organic photodegradation mainly occurs through a semiconductor photocatalysis pathway, except that target substrate, such as oxalate, forms a highly photoactive surface complex with ferric (hydr)oxides.[12,14] The unique evidence for that is the enhanced generation of hydroxyl radicals on the addition of NaF into the aqueous suspension,[14] which is similar to that with the TiO_2 photocatalytic system,[16,17] but it is hardly interpreted by a surface LMCT model. If this holds, the surface complex necessary for LMCT to occur would not be arbitrarily required, and ferric (hydr)oxides as a photocatalyst may find a wide application for treatment of various organic pollutants.

In this paper, we present results of sintering temperature effects on the photocatalytic activity of hematite for degradation of an azo dye, Orange II, in an aqueous suspension under UV irradiation ($\lambda \geq 320$ nm). Hematite (α-Fe_2O_3) is the most stable phase among all ferric (oxyhydr)oxides.[1] Upon thermal treatment, the particle size, surface area, and crystallinity of α-Fe_2O_3 would change, which may then result in changes in the photoactivity and stability toward organic degradation. In the study of splitting water, the poor efficiency of α-Fe_2O_3 photoanodes has been ascribed to a short diffusion length of the photogenerated valence holes (2−20 nm).[18] This hypothesis might be also true for organic reaction using α-Fe_2O_3 as a semiconductor photocatalyst. Therefore, fine particles of α-Fe_2O_3 dispersed on silica were also prepared in parallel as so to minimize particle growth during the sintering process. The photoreactions were carried out in the absence and presence of H_2O_2 at two different initial pHs (3.5 and 6.5). The catalysts were characterized by X-ray powder diffraction, UV/vis diffuse reflectance spectroscopy, FTIR, Raman spectroscopy, surface area, and recycling test to gain information on the catalysts' stability.

2. Experimental Section

Materials. Ferric chloride hexahydrate, silica, Orange II, and hydrogen peroxide in analytical grade were used as received from Shanghai Chemicals Inc. The transparent colloid of ferric oxide was prepared by hydrolysis of ferric chloride (0.3 M) in 0.5 M NaOH at 25 °C, followed by redispersing the precipitates in a ferric chloride solution (0.2 M) at 60 °C for 1 h.[19] The colloidal suspension was then dried at 60 °C with the aid of a rotary evaporator and washed

* To whom correspondence should be addressed. E-mail: xuym@css.zju.edu.cn.

(1) Jolivet, J.-P.; Chaneac, C.; Trone, E. *Chem. Commun.* **2004**, 481–487.
(2) Helz, G. R.; Zepp, R. G.; Crosby, D. G., Eds. *Aquatic and Surface Photochemistry*; Lewis Publishers: Boca Raton, FL, 1994; Chapters 1−3.
(3) Fraust, B. C.; Hoffmann, M. R.; Bahnemann, D. W. *J. Phys. Chem.* **1989**, *93*, 6371–6381.
(4) Siffert, C.; Sulzberger, B. *Langmuir* **1991**, *7*, 1627–1634.
(5) Pehkonen, S. O.; Slefert, R.; Erei, Y.; Webb, S.; Hoffmann, M. R. *Environ. Sci. Technol.* **1993**, *27*, 2056–2062.
(6) Sulzberger, B.; Laubscher, H. *Mar. Chem.* **1995**, *50*, 103–115.
(7) He, J.; Ma, W.; Song, W.; Zhao, J.; Qian, X.; Zhang, S.; Yu, J. C. *Water Res.* **2005**, *39*, 119–128.
(8) Bandara, J.; Mielczarski, J. A.; Lopez, A.; Kiwi, J. *Appl. Catal., B* **2001**, *34*, 321–333.
(9) Mazellier, P.; Bolte, M. *J. Photochem. Photobiol. A* **2000**, *132*, 129–135.
(10) Andreozzi, R.; Caprio, V.; Marotta, R. *Water Res.* **2003**, *37*, 3682–3688.
(11) Bandara, J.; Tennakone, K.; Kiwi, J. *Langmuir* **2001**, *17*, 3964–3969.
(12) Bandara, J.; Mielczarski, J. A.; Kiwi, J. *Langmuir* **1999**, *15*, 7680–7687.
(13) Feng, J.; Hu, X.; Yue, P. L. *Environ. Sci. Technol.* **2004**, *38*, 5773–5778.
(14) Liu, C.; Li, F.; Li, X.; Zhang, G.; Kuang, Y. *J. Mol. Catal. A* **2006**, *252*, 40–48.
(15) Du, W.; Xu, Y.; Wang, Y. *Langmuir* **2008**, *24*, 175–181.
(16) Minero, C.; Mariella, G.; Maurino, V.; Pelizzetti, E. *Langmuir* **2000**, *16*, 2632–2641.
(17) Xu, Y.; Lv, K.; Xiong, Z.; Leng, W.; Du, W.; Liu, D.; Xue, X. *J. Phys. Chem.C* **2007**, *111*, 19024–19032.
(18) Kay, A.; Cesar, I.; Gratzel, M. *J. Am. Chem. Soc.* **2006**, *128*, 15714–15721.

10.1021/la803714m CCC: $40.75
Published on Web 02/06/2009

Table 1. Physical Parameters of the Samples Sintered at Various Temperatures[a]

	Fe_2O_3			Fe_2O_3/SiO_2		
T (°C)	d_s	S_{BET}	E_g	d_s	S_{BET}	E_g
150	16.3	52	2.13	7.1	156 (166)[b]	2.24
200	16.0	48	2.13	8.4	158 (160)	2.12
300	19.3	42	2.13	7.2	140 (163)	2.05
400	24.9	20	2.13	8.4	131 (168)	2.09
500	31.2	15	2.13	14.2	130 (179)	2.20
700	85.6	6	2.13	28.0	111 (159)	2.17
900	>100	1	2.11	70.9	91 (133)	2.16

[a] d_s (nm), crystallite size in diameter; S_{BET}(m^2/g), BET specific surface area; E_g(eV), band gap energy for allowed direct transition. [b] Data in parentheses are the surface area of blank SiO_2.

with water until no chloride was found in the filtrate by silver nitrate. Finally, the solid product was sintered at different temperatures (150−900 °C) for 3 h. Silica-supported ferric oxide (Fe_2O_3/SiO_2) was prepared by mixing an aqueous suspension of silica (33 g/L) with the above colloids of ferric oxide at various ratios. After the mixture was stirred for 1 h, the solid was collected, washed thoroughly with water, and sintered at different temperatures as described above. Experiments for dye photodegradation showed that the optimal loading of Fe_2O_3 on silica was 32.8 wt %. Therefore, this catalyst, denoted as Fe_2O_3/SiO_2, was used for all experiments in comparison with bare Fe_2O_3.

Characterization. FT-IR transmittance spectra were recorded on a Nicolet Nexus 470 instrument. Raman spectra were obtained on a Jobin Yvon LabRam-1B with 632.8 nm He−Ne laser excitation operated at lower than 1 mW. Power X-ray diffraction (XRD) patterns were recorded on a Rigaku D/max-2550/PC diffractometer using Cu Kα1 radiation (0.1540 nm), operated at 40 kV and 250 mA. The crystal structure was identified by the JADE program (hematite, PDF #89-0597; akaganeite, PDF #13-0157). The average crystallite size (d_s) was estimated using the Scherrer equation, based on the (110) and (211) reflections of hematite and akaganeite, respectively. Diffuse reflectance spectra were recorded on a Shimadzu UV2550 spectrometer and referenced to $BaSO_4$. The band gap energy of ferric oxide (E_g) for the allowed direct transition was estimated by following the procedure described by Chaudhuri and co-workers.[20] The Brunauer−Emmett−Teller (BET) specific surface area (S_{BET}) was measured on a Micromeritics ASAP2020 apparatus by N_2 adsorption at 77 K. These data (d_s, E_g, and S_{BET}) are summarized in Table 1.

Reactions and Analysis. The reactor was made of Pyrex glass with a water jacket. The light source was a Xenon lamp (75 W, USHIO), enclosed in an A1010 lamp housing and operated at 5.00 A (LPS 200, PTI). Typically, 25 mg of solid and 50.0 mL of dye aqueous solution (0.10 mM) were mixed and stirred magnetically in the dark for 4 h. After equilibrium, about 2 mL of the suspension was withdrawn by a syringe and filtered through a membrane (pore size 0.22 μm, Shanghai XingYa). The dye concentration remaining in the filtrate was analyzed at 483 nm on an Agilent 8451 spectrometer. The decrease in dye concentration was used for calculation of the dye adsorption, q_e, in unit of moles per gram of catalyst. The residual suspension (48 mL) was irradiated with UV light ($\lambda \geq 320$ nm) under a constant stirring. At given intervals, small aliquots were withdrawn by syringe and filtered through a membrane. The dye concentration in the filtrate was measured at 483 nm by the standard photometric method. Total dissolved iron species in solution was analyzed at 512 nm through a Fe(II) complex with 1,10-phenathroline. Before the measurement, Fe(III) species was reduced in advance by hydroxylamine hydrochloride.[21]

The photonic efficiency[22] was calculated by the equation, $\zeta = R/I_0$, where R and I_0 are the rate of dye degradation and the incident photon flux at a given wavelength. The measurement was made with an interference filter (385 ± 13 nm, 25 mm in diameter, Shanghai Haiguang Optics). The experimental conditions were the same as those described above (i.e., 50 mL of 0.10 mM dye solution, and 0.50 g/L of catalyst). The light intensity entering into the reactor was measured, by using ferric oxalate actinometry,[23] as 5.87×10^{-7} einsteins/min.

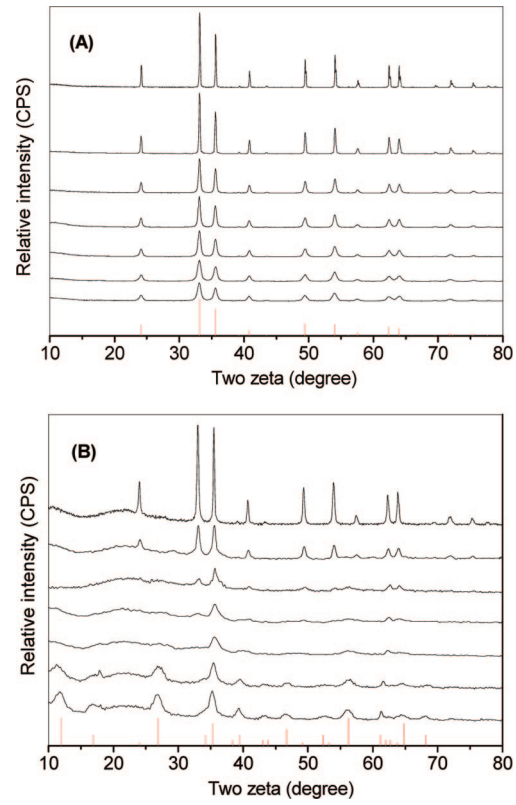

Figure 1. XRD patterns of (A) Fe_2O_3 and (B) Fe_2O_3/SiO_2, sintered at 150, 200, 300, 400, 500, 700, and 900 °C (from bottom to top). The red lines in parts A and B are the standard XRD patterns of α-Fe_2O_3 (PDF #89-0597) and β-FeOOH (PDF #13-0157), respectively.

3. Results and Discussion

Characterization of the Samples. Figure 1 shows the XRD patterns of Fe_2O_3 and Fe_2O_3/SiO_2 sintered at various temperatures. In the absence of silica (Figure 1A), all samples display the same patterns as those of α-Fe_2O_3 (PDF #89-0597). However, in the presence of silica (Figure 1B), only the samples sintered at a temperature higher than 200 °C show a similar diffraction to α-Fe_2O_3, whereas the samples sintered at low temperature (150 and 200 °C) give a pattern characteristic of β-FeOOH (PDF #13-0157). A separate experiment showed that the parent ferric oxide colloids, used for the synthesis of both Fe_2O_3 and Fe_2O_3/SiO_2, were in fact a mixture of NaCl and β-FeOOH crystallites. The result illustrates that the phase transformation from β-FeOOH to α-Fe_2O_3 upon thermal treatment[1] is inhibited on silica. Moreover, the (110) peak at $2\theta = 35.6°$ appears to be stronger than the (104) peak at $2\theta = 33.1°$ (Figure 1B), relative to unsupported α-Fe_2O_3 (Figure 1A). This may indicate a preferential orientation of the (110) axis vertical to the silica surface, as suggested by Grätzel and co-workers.[18]

As the sintering temperature is increased, the peaks become more and more acute and intensive with both sets of the samples

(19) Sugimoto, T.; Wang, Y.; Itoh, H.; Muramatsu, A. *Colloids Surf. A* **1998**, *134*, 265–279.
(20) Chakrabarti, S.; Ganguli, D.; Chaudhuri, S. *Physica E* **2004**, *24*, 333–342.
(21) Tamura, H.; Goto, K.; Yotsuyanagi, T.; Nagayama, M. *Talanta* **1974**, *21*, 314–318.
(22) Serpone, N. *J. Photochem. Photobiol. A* **1997**, *104*, 1–12.
(23) Rabek, J. F. *Experimental Methods in Photochemistry and Photophysics*; John Wiley Sons: New York, 1982; Part 2, p 944.

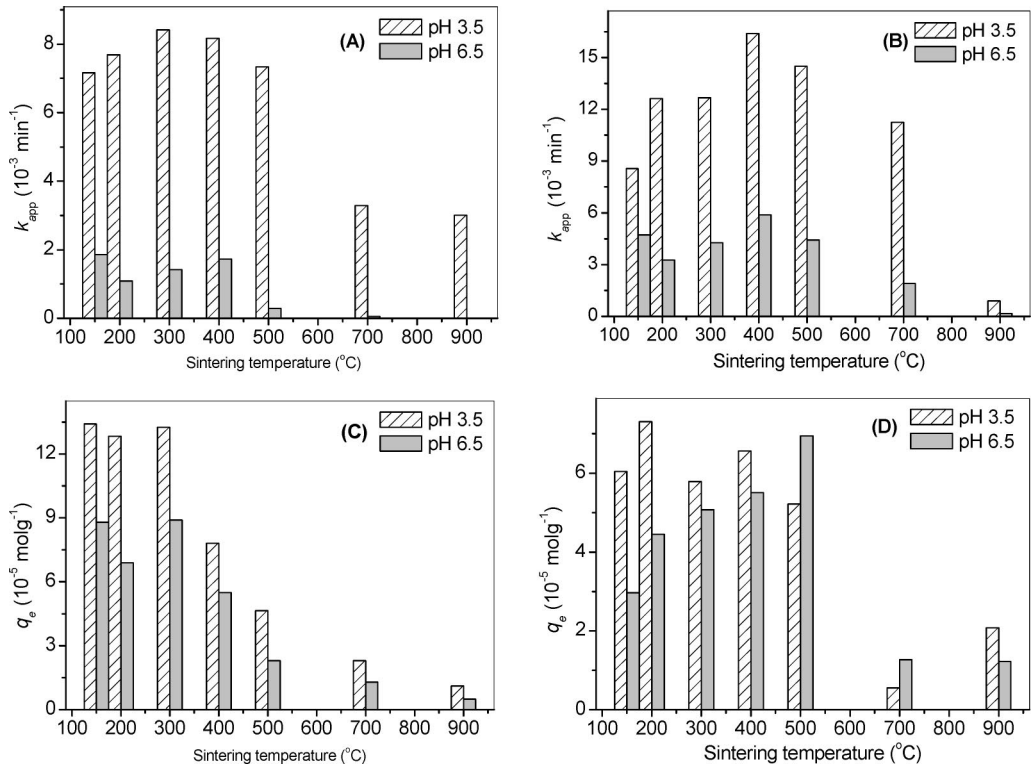

Figure 2. Effect of sintering temperature on the apparent rate constant of dye photodegradation (k_{app}) and on the initial amount of dye adsorption (q_e), in the aerated aqueous suspension of (A, C) Fe_2O_3 and (B, D) Fe_2O_3/SiO_2. The initial pH of the dye solution was set at 3.5 and 6.5, respectively.

(Fe_2O_3 and Fe_2O_3/SiO_2). This presumably indicates an increase in the size and crystallinity of the elementary crystallites (β-FeOOH and α-Fe_2O_3). The average size of these nanocrystals (d_s) was then estimated from the peak broadening using the Scherrer equation, and the results are listed in Table 1. A progressive increase in the crystallite size with increasing sintering temperature is obvious. Also, the α-Fe_2O_3 crystallites supported on silica appear to be smaller than those of unsupported α-Fe_2O_3 sintered at the same sintering temperature. Such a trend in the particle size was also evidenced by the BET specific surface area measured with N_2 adsorption at 77 K (Table 1). As the sintering temperature is increased, the surface area is decreased correspondingly with both sets of the samples. The Fe_2O_3/SiO_2 samples have a higher surface area than the α-Fe_2O_3 samples, mainly due to the presence of high surface silica. Provided that silica has a similar area before and after loading with ferric oxide, the surface area ascribed to the neat ferric oxide in Fe_2O_3/SiO_2 may be estimated. This surface area per gram of the loaded ferric oxide (not shown) is indeed larger than that of unsupported α-Fe_2O_3, and the value also shows an expected decrease with increasing sintering temperature. The result indicates that silica not only functions as a phase stabilizer but also as a dispersing reagent for fine ferric oxide particles.

FTIR, Raman, and UV−visible diffuse reflectance spectra of these samples were also measured (Figures S1 and S2, Supporting Information). The vibration bands of Fe_2O_3/SiO_2 were nearly the same as those of individual α-Fe_2O_3 and SiO_2, but the vibration of α-Fe_2O_3 at 552 cm^{-1} was gradually shifted to 581 cm^{-1} as the SiO_2 loading was increased. This may indicate formation of a Fe−O−Si bond between α-Fe_2O_3 and silica.[24] However, the Raman spectra did not show such information on the Fe−O−Si bond (only the vibrations due to α-Fe_2O_3[25] were observed). In the UV−vis absorption spectra, all the samples exhibited a broad band mainly in the region from 200 to 600 nm. The band gap energy for allowed direct transition was then estimated, which was about 2.1−2.2 eV (Table 1), in good agreement with the literature value of 2.2 eV for α-Fe_2O_3.[26]

Effect of Sintering Temperature on the Photoactivity. The catalyst photoactivity was evaluated in aqueous suspension under UV light irradiation ($\lambda \geq 320$ nm), by using Orange II as a model substrate. Previous study has shown that this anionic azo dye adsorbs strongly and degrades easily on Fe_2O_3 in an acidic aqueous suspension.[11,15] The change of dye concentration in solution with irradiation time was well-fitted into the first-order kinetic equation (Figure S3, Supporting Information). Figure 2 compares the relevant rate constants (k_{app}), obtained with Fe_2O_3 and Fe_2O_3/SiO_2 sintered at various temperatures in an aerated aqueous suspension at different initial pHs. In this figure is also included the initial amount of dye adsorption (q_e) measured in the dark and before the photoreaction.

There appear several trends in Figure 2. First of all, the rate constant of dye photodegradation increases first and then decreases as sintering temperature is increased. The optimal temperature is about 400 °C for both Fe_2O_3 and Fe_2O_3/SiO_2. Second, the rate constants obtained at initial pH 3.5 are larger than those at initial pH 6.5. Third, the rate constants measured with Fe_2O_3/SiO_2 are larger than those obtained with Fe_2O_3 under similar conditions. On the other hand, the initial amount of dye adsorption is also a function of sintering temperature and initial pH. The dye dark adsorption is higher at initial pH 3.5 than that at initial pH 6.5 and is higher on Fe_2O_3 than on Fe_2O_3/SiO_2. The former is ascribed to more positive surface charges on Fe_2O_3 at lower pH for uptake

(24) Predoi, D.; Crisan, O.; Jitianu, A.; Valsangiacom, M. C.; Raileanu, M.; Crissan, M.; Zaharescu, M. *Thin Solid Films* **2007**, *515*, 6319–6323.

(25) Froment, F.; Tournie, A.; Colomban, P. *J. Raman Spectrosc.* **2008**, *39*, 560–568.

(26) Sherman, D. M. *Geochim. Cosmochim. Acta* **2005**, *69*, 3249–3255.

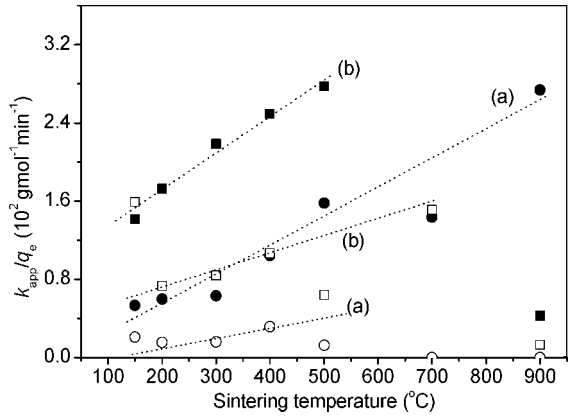

Figure 3. Adsorption-normalized rate constant of dye photogradation as a function of sintering temperature for (a) Fe_2O_3 and (b) Fe_2O_3/SiO_2 at an initial pH of 3.5 (solid bars) and 6.5 (open bars). The dotted lines were only made as a reference.

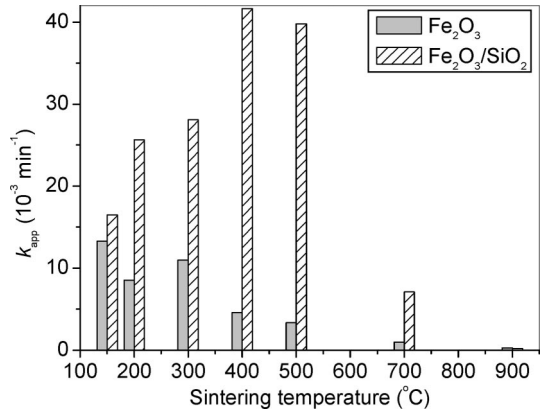

Figure 4. Effect of sintering temperature on the apparent rate constant of dye photodegradation in the presence of H_2O_2 (1.2 mM) at initial pH 6.5 over Fe_2O_3 and Fe_2O_3/SiO_2.

of anionic dye. The latter is due to the fact that there is only 32.8% Fe_2O_3 in the Fe_2O_3/SiO_2 sample, and the silica surface is negatively charged under present conditions (the pH at the zero point charge is 8.9 for α-Fe_2O_3[26] and 2−3 for SiO_2). However, the dye adsorption on Fe_2O_3/SiO_2 displays some irregular change with sintering temperature, especially at initial pH 6.5. Separate experiment showed that silica particles underwent hydrolysis to give a final pH of 3.6. Besides experimental error, the sintering temperature may be a factor influencing the degree of silica hydrolysis.

The photonic efficiency[22] was estimated at $\lambda = 385 \pm 13$ nm for the samples sintered at 400 °C. The results obtained at initial pH 6.5 and 3.5 were 0.019% and 0.056% for Fe_2O_3 and 0.043% and 0.10% for Fe_2O_3/SiO_2, respectively. The ζ value is larger with Fe_2O_3/SiO_2 than that with Fe_2O_3, and it is also larger at initial pH 3.5 than that at initial pH 6.5. This trend of ζ at $\lambda = 385 \pm 13$ nm is essentially the same as that of k_{app} measured at $\lambda \geq 320$ nm for these catalysts. Note that the ζ values are only taken as a low limit of photonic efficiency, since the incident photons entering into the reactor are seriously scattered by the suspended particles in the aqueous solution.

It is known that the rate of photodegradation of Orange II on ferric (hydr)oxide is proportional to its surface concentration at monolayer.[11,15] For this concern, the adsorption-normalized rate constant (k_{app}/q_e) as a function of sintering temperature is shown in Figure 3. It is interesting to see that, for both Fe_2O_3 and Fe_2O_3/SiO_2, the adsorption-normalized rate increases almost linearly with the sintering temperature up to at least 500 °C (some data are highly scattered, mainly due to weak adsorption of dye on the catalyst sintered at high temperature). This specific rate can be taken as a measure of the relative activity among different photocatalysts. The result is in agreement with the model of semiconductor photocatalysis proposed previously.[15] As sintering temperature is increased, the catalyst becomes better crystallized (Figure 1), and the number of defect sites would be reduced.[27,28] This would result in a decreased rate of recombination of photogenerated charge carriers, thus accelerating the dye degradation via valence holes on Fe_2O_3.[15] Second, both Fe_2O_3 and Fe_2O_3/SiO_2 show a higher photocatalytic activity at initial pH 3.5 than at initial pH 6.5. The flat-band potential of α-Fe_2O_3 is pH-dependent.[26,29] A more positive redox potential at lower pH would favor the interfacial electron transfer for dye degradation. Third, Fe_2O_3/SiO_2 shows a higher photocatalytic activity than Fe_2O_3 under similar conditions. This may relate to the fact that the α-Fe_2O_3 crystallites on silica have a smaller average size than the unsupported α-Fe_2O_3 (Table 1). In the study of splitting water, the poor efficiency of α-Fe_2O_3 photoanode has been ascribed to a short diffusion length of the photogenerated valence holes (2−20 nm).[18] This hypothesis may also be applicable for the present work. Otherwise, the observed difference between α-Fe_2O_3 and Fe_2O_3/SiO_2 might be ascribed to the dissolved ferric species, whose photolysis may initiate dye degradation. For this concern, two filtrate solutions were prepared from the aqueous suspensions at pH 3.5 of Fe_2O_3 and Fe_2O_3/SiO_2 (both sintered at 400 °C). However, in such filtrate solutions, the dye photolysis was very slow ($k_{app} = 1.0 \times 10^{-3}$ min^{-1}).

It is worth noting that β-FeOOH supported on SiO_2 is also photoreactive for dye degradation. According to our knowledge, this is the first time it is reported in the literature. To date, all available ferric (hydr)oxides have been proven to be photoactive for organic degradation in aqueous suspension, including α-, β-, δ-, γ-FeOOH; Fe_3O_4; and α-, γ-Fe_2O_3.[4−15]

Effect of H_2O_2 Addition. It is known that the addition of H_2O_2 into the aqueous suspensions of ferric (hydr)oxides can result in enhancement in the rate of dye photodegradation, ascribed to the combined effects of conduction electron scavenging and the Fenton reaction.[15] Then, it is necessary to examine whether the H_2O_2 effect is dependent on sintering temperature. Figure 4 shows the result of dye photodegradation with Fe_2O_3 and Fe_2O_3/SiO_2 in the presence of H_2O_2 at initial pH 6.5. All the reaction rates are significantly increased on the addition of H_2O_2, as compared to those only in an aerated aqueous suspension (Figure 2). However, as sintering temperature is increased, the degree of rate enhancement (i.e., the ratio of rate constant in the presence of H_2O_2 to that in the absence of H_2O_2) is first increased and then decreased, the trend of which (data not shown) is similar to that presented in Figure 3. The maximal rate enhancement appears at 500 °C for both Fe_2O_3 and Fe_2O_3/SiO_2. This is reasonable, since the catalyst photocatalytic activity is the cause, and H_2O_2 is only the effect. On those catalysts sintered at 900 °C, the dye adsorption was very weak, and thus, the dye degradation was very slow, even in the presence of H_2O_2. This implies that the H_2O_2-promoted dye degradation mainly occurs on the surface of irradiated catalyst, not in solution, consistent with the previous observation.[15]

(27) Hoffmann, M. R.; Martin, S. T.; Choi, W.; Bahnemann, D. W. *Chem. Rev.* **1995**, *95*, 69–96.
(28) Carp, O.; Huisman, C. L.; Reller, A. *Prog. Solid State Chem.* **2004**, *32*, 33–177.
(29) Leland, J. K.; Bard, A. J. *J. Phys. Chem.* **1987**, *91*, 5076–5083.

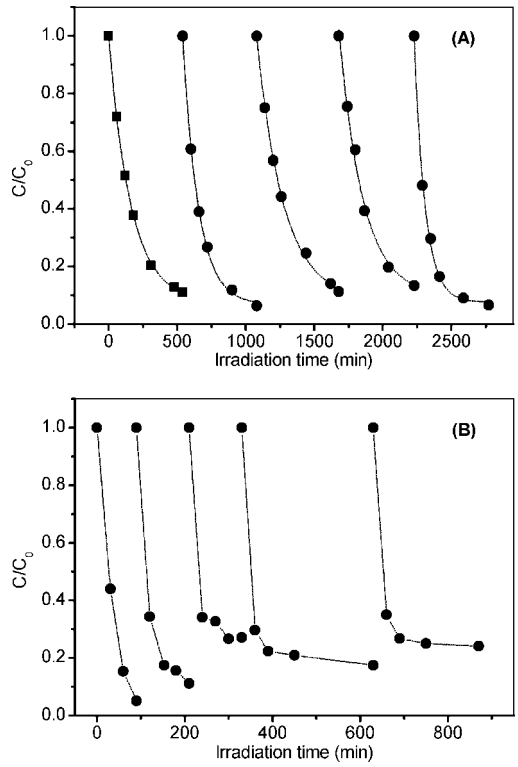

Figure 5. Recycling degradation of Orange II as a function of irradiation time in the presence of H_2O_2, obtained with (A) Fe_2O_3 and (B) Fe_2O_3/SiO_2 sintered at 400 °C. Conditions: catalyst, 1.50 g/L; dye solution, 1.0 mM/each run, pH 6.5; H_2O_2, 1.20 mM/each run.

Photostabilities of Fe_2O_3 and Fe_2O_3/SiO_2. The photoinduced reductive dissolution of ferric (hydr)oxide is a question to be answered for possible water treatment. Figure 5 shows the results of recycling experiments for dye photodegradation in the presence of H_2O_2, obtained with Fe_2O_3 and Fe_2O_3/SiO_2 (both sintered at 400 °C). During five consecutive runs, the rate of dye degradation with Fe_2O_3 remains nearly unchanged. However, the rate with Fe_2O_3/SiO_2 is decreased notably from one run to another. It is noted that the total reaction time with Fe_2O_3 is 45 h, but it is only 15 h with Fe_2O_3/SiO_2. After the recycling, the total dissolved iron species was measured to be 39 μM for Fe_2O_3 and 89 μM for Fe_2O_3/SiO_2, whereas the suspension pH was decreased to 3.7 for both the systems. Although the photodissolution is obvious, the accumulated iron species in aqueous phase only accounts for 0.2% of Fe_2O_3 and 1.4% of Fe_2O_3/SiO_2 used for the test.

The photodissolution process may lead to a change in the solid crystalline structure. For this concern, all the particles were collected, dried at 60 °C, and analyzed by XRD. In these samples, new crystalline phase were not found except α-Fe_2O_3 (the Raman measurement was failed due to a fluorescence problem). However, the (100) peak intensity was decreased by 7% for α-Fe_2O_3 and 17% for α-Fe_2O_3/SiO_2, relative to several control samples (Table 2). In addition, the average size of α-Fe_2O_3 crystallites was also increased somewhat, from 30.6 to 33.1 nm for α-Fe_2O_3 and from 8.4 to 8.8 nm for α-Fe_2O_3/SiO_2. This presumably indicates that the finer crystallites photodissolve faster than the larger particles. Then the dissolved ferric species are redeposited onto α-Fe_2O_3, followed by surface reconstruction. In the presence of silica, such deposition would preferably occur on SiO_2, due to the negatively charged surface of silica under the experimental conditions. The newly formed ferric (hydr)oxide on silica is mostly amorphous and less photoactive than is the crystalline ferric (hydr)oxides. This hypothesis may account for the observation that α-Fe_2O_3/SiO_2 is more photoactive but less stable than α-Fe_2O_3 for dye degradation.

Table 2. XRD Data for the Samples Treated at Different Conditions[a]

samples	I_{110}	A_{110}	d_p (nm)
Fe_2O_3 + H_2O + dark	2913	54 823	30.6
Fe_2O_3 + H_2O + $h\nu$	2711	53 934	30.4
Fe_2O_3 + dye + $h\nu$	2752	53 886	33.1
Fe_2O_3/SiO_2 + H_2O +dark	379	21 218	8.4
Fe_2O_3/SiO_2 + H_2O + $h\nu$	376	20 554	8.6
Fe_2O_3/SiO_2 + dye + $h\nu$	315	16 788	8.8

[a] I_{100}, the (110) peak intensity; A_{100}, the (110) peak integrated area; d_s (nm), crystallite size in diameter. Experiments were made in parallel under similar conditions. After each reaction, the suspensions were filtered through a membrane filter (0.22 μm in pore size), and the particles were directly dried at 60 °C in a vacuum oven, followed by the XRD analysis.

4. Conclusions

This work has shown that the photocatalytic activities of both α-Fe_2O_3 and α-Fe_2O_3/SiO_2 increase with the sintering temperature up to 500 °C at least. The catalysts also appear to be more photoactive with finer crystallites and at lower pH, even though a systematic study is still needed. Experimental evidence are well explained in terms of the semiconductor photocatalysis. On the other hand, the photoinduced reductive dissolution of ferric oxide, especially in the presence of organic dye, is obvious, but it is not as serious as previously though. This is probably due to surface redeposition and reconstruction of the dissolved iron species onto α-Fe_2O_3. The stability of α-Fe_2O_3/SiO_2 is poor and ascribed to silica's affinity toward the dissolved iron species. The outstanding stability of bare α-Fe_2O_3 against photodissolution in a weakly acidic solution makes it worthy of further development as a photocatalyst for water treatment.

Acknowledgment. This work was supported by the National Natural Science Foundation of China (Nos. 20525724, and 20873124) and the National Basic Research Program of China (No. 2009CB825300).

Supporting Information Available: Figures S1−S3. This material is available free of charge via the Internet at http://pubs.acs.org.

LA803714M